Superconductivity, incoherence and Anderson localization in the crystalline organic conductor $(BEDT\text{-}TTF)_3Cl_2\cdot 2H_2O$ at high pressures

2002 J. Phys.: Condens. Matter 14 7345

(http://iopscience.iop.org/0953-8984/14/31/306)

INSTITUTE OF PHYSICS PUBLISHING JOURNAL OF PHYSICS: CONDENSED MATTER

J. Phys.: Condens. Matter **14** (2002) 7345–7361 PII: S0953-8984(02)35210-X

Superconductivity, incoherence and Anderson localization in the crystalline organic conductor (BEDT-TTF)$_3$Cl$_2$·2H$_2$O at high pressures

Paul Goddard[1,4], **Stanley W Tozer**[2], **John Singleton**[1], **Arzhang Ardavan**[1], **Adam Abate**[2] **and Mohamedally Kurmoo**[3]

[1] Clarendon Laboratory, Oxford University, Parks Road, Oxford OX1 3PU, UK
[2] National High Magnetic Field Laboratory, 1800 East Paul Dirac Drive, Tallahassee, Florida, FL 32310, USA
[3] IPCMS, 23 rue du Loess, BP 20/CR, 67037 Strasbourg Cedex, France

E-mail: p.goddard@physics.ox.ac.uk

Received 26 March 2002
Published 24 July 2002
Online at stacks.iop.org/JPhysCM/14/7345

Abstract

The conducting properties of the pressure-induced, layered organic superconductor (BEDT-TTF)$_3$Cl$_2$·2H$_2$O have been studied at 13.5 and 14.0 kbar using low temperatures, high magnetic fields and two-axis rotation. An upper critical field that is significantly larger than that expected from the Pauli paramagnetic limit is observed when the field is applied parallel to the conducting layers. The angle-dependent magnetoresistance suggests incoherent transport between the conducting layers at both pressures and the observed negative magnetoresistance at 13.5 kbar can be explained by considering Anderson localization within the layers. Further application of pressure destroys the effects of localization.

(Some figures in this article are in colour only in the electronic version)

1. Introduction

The study of electrically conducting crystalline materials made from organic molecules is an increasingly large and active area of research. The high degree of anisotropy and the strong electron–electron interactions in these crystalline organic conductors means that they can possess a wide variety of ground state phases [1]. Of particular interest are the class of organic conductors which exhibit superconductivity, and the similarities between these and the 'high-T_c' cuprate superconductors are well documented [2].

One family of such organic conductors is made using the charge transfer salts of the organic molecule bis(ethlyene-dithio)tetrathiafulvalene (BEDT-TTF). These tend to be layered

[4] Author to whom any correspondence should be addressed.

materials with highly conducting planes of the BEDT-TTF molecules separated by anion layers (for a complete overview see [1, 3]). Understanding the nature of the interlayer transport in these materials is important in achieving a grasp of the interactions that cause the superconductivity, which in many cases is thought to be non-BCS-like [4]. In a pressure and temperature phase diagram the superconducting state is frequently adjacent to a density-wave state caused by nesting of quasi-one-dimensional (Q1D) pieces of the Fermi surface, and this leads to the suggestion that superconductivity is mediated by density wave fluctuations. The topology of the Fermi surface will obviously have an effect on its nesting properties. Thus measurements that investigate the nature of the interlayer transport in these materials are of particular significance, as coherent transport between the layers necessitates the existence of a three-dimensional, rather than two-dimensional, Fermi surface [5].

(BEDT-TTF)$_3$Cl$_2$·2H$_2$O is so far unique in this family of organic crystal in that each of the BEDT-TTF ions has an average charge of $+\frac{2}{3}e$. Band calculations suggest that at room temperature and ambient pressure this material should be a semimetal [6, 7], and thermopower and conductivity measurements confirm this [8]. As the temperature is reduced below $T \approx 160$ K (BEDT-TTF)$_3$Cl$_2$·2H$_2$O undergoes a (semi)metal–insulator transition into a charge-density-wave (CDW) state [9]. A further Fermi surface reconstruction occurs at $T \approx 60$ K and the sample then remains insulating down to very low temperatures. The application of hydrostatic pressure suppresses the onset of the density-wave state, and at 10.2 kbar a superconducting state is formed with $T_c = 4$ K. In their paper Lubczynski *et al* [10] observe that the onset of superconductivity coincides with a saturating magnetoresistance in fields of up to 15 T. They suggest that this implies it is quasi-two-dimensional (Q2D) carriers that are responsible for the superconducting transport. Lubczynski *et al* [10] also show that as the pressure is increased further the CDW transition is completely suppressed causing the liberation of the Q1D carriers and yielding a non-saturating magnetoresistance. Superposed over the top of this magnetoresistance they observe low-amplitude, low-frequency Shubnikov–de Haas (SdH) oscillations, indicating that the Q2D carriers are still present. Lubczynski *et al* go on to state that if the pressure is still further increased above 14 kbar the superconducting state is destroyed and the material becomes metallic. Figure 1 shows the phase diagram shown in [10] and first proposed in [11].

2. Experimental details

2.1. Sample properties

(BEDT-TTF)$_3$Cl$_2$·2H$_2$O crystallizes in the triclinic space group $P\bar{1}$, with $a = 11.214 \pm 0.002$ Å, $b = 13.894 \pm 0.002$ Å, $c = 15.924 \pm 0.002$ Å, $\alpha = 94.74 \pm 1°$, $\beta = 109.27 \pm 1°$ and $\gamma = 97.03 \pm 1°$ [12]. The conducting planes of the (BEDT-TTF) molecules lie in the ab-plane with the long axis of the molecules lying approximately parallel to the c-axis (see figure 2).

Using their electronic band structure calculation Whangbo *et al* suggest that the in-plane Fermi surface of (BEDT-TTF)$_3$Cl$_2$·2H$_2$O at room temperature and pressure consists of an elongated closed electron pocket centred at the corner of the Brillouin zone, together with an open electron Fermi surface and an open hole Fermi surface oriented along the Γ–Y (b^*) direction (see figure 2) [6]. As already mentioned, the material is a semimetal at room temperature and the ratio of resistivities along the crystal axes a, b and c is ρ_a:ρ_b:ρ_c = 1:7:1000 [7].

The high purity, single-crystal samples of (BEDT-TTF)$_3$Cl$_2$·2H$_2$O are grown electrochemically using quenched-recrystallized BEDT-TTF from chloroform, and recrystallized tetraethylammonium chloride from ethanol. The solvent used was distilled

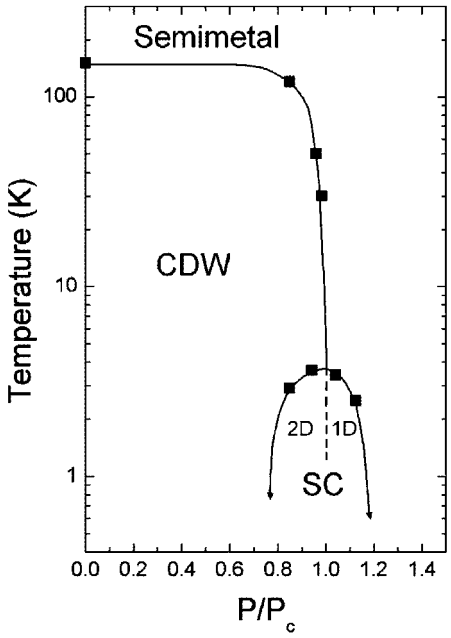

Figure 1. The phase diagram of $(BEDT\text{-}TTF)_3Cl_2{\cdot}2H_2O$ proposed by Lubczynski *et al* [10]. P_c is the critical pressure at which the onset of the CDW state tends to zero temperature and the pressure that separates the region of saturating magnetoresistance from the region of diverging magnetoresistance in fields of up to 15 T as shown by the dotted line. In [10] P_c is found to be close to 12 kbar.

HPLC grade dichloromethane. The electrocrystallization was performed at 0.5 μA for three months. To ensure high purity, especially of the surface, the crystallization was stopped when 50% of the BEDT-TTF was consumed. The resulting single crystals are black platelets generally of the order of $2 \times 2 \times 0.05$ mm^3 with the plane of the plate corresponding to the highly conducting layers. The sample used in this paper was cleaved so that it would fit in a pressure cell and measured $120 \times 100 \times 45$ μm^3.

2.2. Two-axis rotation at high hydrostatic pressure

The experiments described in this paper involve rotation of the $(BEDT\text{-}TTF)_3Cl_2{\cdot}2H_2O$ sample about two axes in a high magnetic field at pressures of 13.5 ± 0.1 and 14.0 ± 0.1 kbar. These pressures were achieved using the turnbuckle diamond anvil pressure cell (DAC) shown in figure 3(a). This DAC was designed and built in the National High Magnetic Field Laboratory (NHMFL), Tallahassee and consists of two natural diamonds enclosed in a body of high-tensile BeCu [13]. The highly polished, flat faces of the diamonds are separated by a 65 μm thick, stainless steel gasket coated in alumina. Two wires of pressed gold are attached to each of the two broad faces of the sample using a paste made from a mixture of graphite and gold. The sample is then placed inside a cavity in the gasket, which is filled with a liquid pressure medium, in this case glycerine. The DAC is then assembled with the sample wires being electrically contacted to wires that emerge from the cell body and the required room temperature pressure is applied using a hydraulic press. Prior to removal from the press the pressure can be maintained by means of a screw-type locking mechanism. Figure 3(b) shows the sample used in this paper in position on the DAC, prior to assembly.

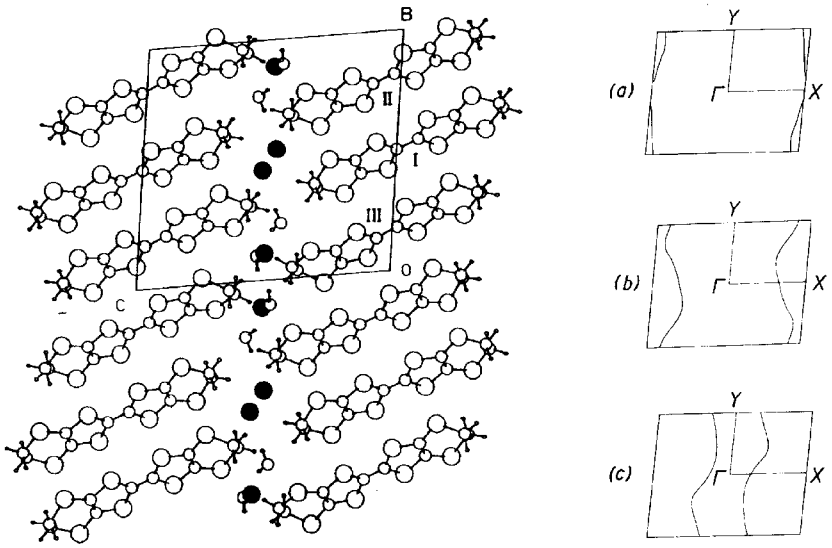

Figure 2. Left: view of the unit cell of $(BEDT\text{-}TTF)_3Cl_2{\cdot}2H_2O$ along the a-axis. It consists of three independent BEDT-TTF molecules, two chlorine atoms and two water molecules. Six BEDT-TTF molecules collectively donate four electrons to each anion leaving each molecule with an average charge of $+\frac{2}{3}e$ (from [12]). Right: the Fermi surface of Whangbo *et al* [6]; (a) shows the Q2D closed electron pocket, (b) the Q1D electron sheet and (c) the Q1D hole sheet.

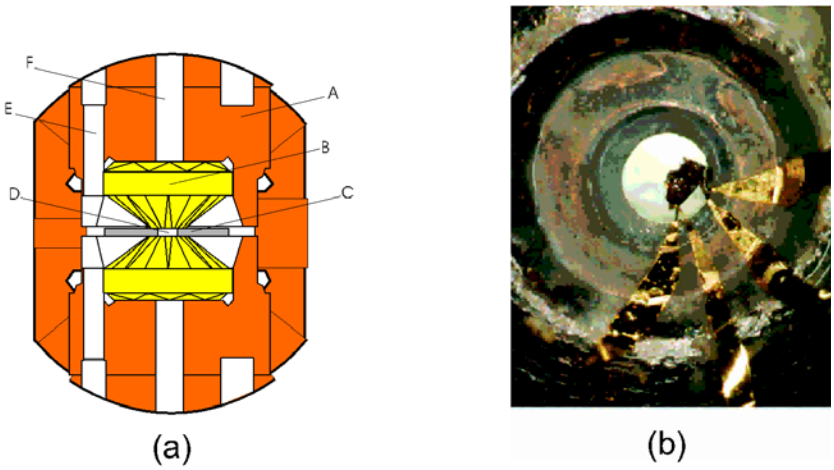

Figure 3. (a) Diagram of the turnbuckle DAC with outer diameter 6.4 mm. A: threaded end cap. B: upper diamond. C: stainless steel gasket. D: sample cavity. E: feedthrough for sample wires. F: light well used to deliver radiation for exciting the ruby fluorescence used in calibrating the pressure. (b) The $(BEDT\text{-}TTF)_3Cl_2{\cdot}2H_2O$ sample in position in the gasket cavity prior to assembly. The cavity diameter is 350 μm.

The magnetoresistance measurements were made using standard four-wire AC techniques ($f \sim 80$ Hz) with the current applied in the interplane direction ($I = 1$–25 μA).

The pressure inside the sample cavity is calibrated by comparing the fluorescence of a fragment of ruby located alongside the sample in the DAC and the fluorescence of another fragment at the same temperature, but ambient pressure [15]. This is measured using a helium-

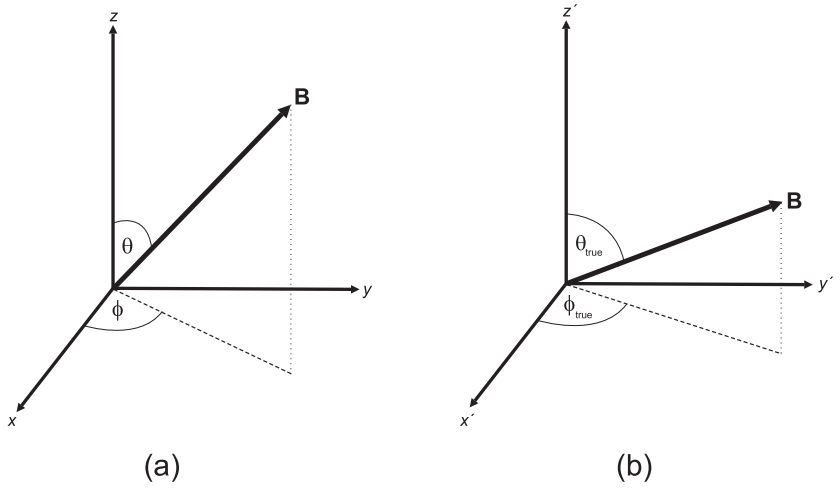

Figure 4. (a) The laboratory frame, showing the relation between θ, ϕ and the magnetic field, $\boldsymbol{B}$. The z-axis corresponds to the long axis of the DAC. (b) The sample frame, showing the relation between $\theta_{\rm true}$, $\phi_{\rm true}$ and the magnetic field. The z'-axis corresponds to the normal to the ab-planes.

cadmium laser and a charge-coupled device detector. The shift in wavelength of the ruby R_1 fluorescence line as a function of pressure is well known [14, 15] and independent of temperature. Thus the pressure in the sample cavity can be found at any temperature.

The two-axis rotation was achieved using an insert designed and built in Oxford. The angle between the normal to the ab-planes and the magnetic field (the θ-angle) can be varied continuously via a motor and worm-drive arrangement and measured using a potentiometer. The in-plane, or azimuthal angle (the ϕ-angle) can be changed in discrete steps using a retractable rod that travels along the axis of the rotator. This should enable the B-field to be directed along all possible sample directions.

All measurements were performed at NHMFL, Tallahassee at temperatures of 500 mK and in fields of up to 33 T.

2.3. Effect of sample misalignment

It is possible in experiments such as those presented here that the sample axes are not accurately aligned, i.e. that the normal to the ab-planes is inclined at an unknown angle to the long axis of the DAC. This is especially true when the sample is located within a pressure cell for a number of reasons. Probably most important of these is the forces that act on the sample as the temperature is reduced and the pressure medium freezes. The necessity of having extremely thin contact wires means that the sample will move easily under even small forces. Another origin of this misalignment comes from the difficulty in cleaving these samples to be so small. After cleaving it is not possible to guarantee that the plane of the sample corresponds exactly to the ab-planes. Whatever the cause, this offset means that the measured θ and ϕ-angles are not the true angles associated with the sample ($\theta_{\rm true}$ and $\phi_{\rm true}$). In fact changing *either* of the measured angles will change *both* $\theta_{\rm true}$ *and* $\phi_{\rm true}$.

In the general situation shown in figure 4, we measure the angles θ and ϕ (in the laboratory frame) and we wish to know the angles $\theta_{\rm true}$ and $\phi_{\rm true}$ (in the sample frame). The difference between these two sets of angles is due to a misalignment of the two frames by an unknown

angle in an unknown direction such that the angle between the z- and z'-axes is ϵ and the angle between the x-axis and the projection of the x'-axis onto the xy-plane is ψ. Writing down the transformation matrix for converting the laboratory into the sample frame leads us to the following equations for θ_{true} and ϕ_{true}:

$$\cos\theta_{\text{true}} = \sin\theta\sin\epsilon\cos(\phi-\psi) + \cos\theta\cos\epsilon \tag{1}$$

$$\cos\phi_{\text{true}} = \frac{\sin\theta\cos\epsilon\cos(\phi-\psi) - \cos\theta\sin\epsilon}{\sin\theta_{\text{true}}} \tag{2}$$

$$\sin\phi_{\text{true}} = \frac{\sin\theta\sin(\phi-\psi)}{\sin\theta_{\text{true}}}. \tag{3}$$

For a highly anisotropic, layered superconductor like (BEDT-TTF)$_3$Cl$_2$·2H$_2$O the upper critical field (B_{c2}) has a maximum when the magnetic field is in the ab-planes ($\theta_{\text{true}} = 90°$) [16, 17]. Thus if we set the magnetic field to be just below this maximum B_{c2}, but above the field required for zero resistance, then we observe a sharp minimum in the resistance when we rotate the sample in a magnetic field. The minimum in resistance occurs when the sample is exactly in the plane of the sample [18]. Setting $\theta_{\text{true}} = 90°$ in equation (1) gives

$$\cot\theta = -\tan\epsilon\cos(\phi-\psi). \tag{4}$$

Fitting this equation to a plot of the θ positions of the resistance minima against ϕ yields values for the constants ϵ and ψ. Substituting these values into equations (1)–(3) gives a function for θ_{true} that is single valued over the range $0 < \theta_{\text{true}} < 180°$ and a function for ϕ_{true} that is single valued over 360°.

It is worth noting that as a result of this misalignment it is not possible to access the $\theta_{\text{true}} = 0°$ and 180° directions for a given ϕ except when $\phi = \psi$.

3. Results and discussion

3.1. Anisotropy of the upper critical field

At both pressures measured in these studies the (BEDT-TTF)$_3$Cl$_2$·2H$_2$O sample undergoes a transition into a superconducting state at low temperatures. The T_c-values at 13.5 and 14.0 kbar are found to be 3.5 ± 0.5 and 2.6 ± 0.5 K respectively, where T_c is defined by the midpoint of the resistive transition. A study of the angular dependence of the upper critical field (B_{c2}) at each pressure was made by sweeping the field at fixed θ_{true}-angles and using linear extrapolation to extract B_{c2} as shown in figure 5. For a discussion of why this method of extracting B_{c2} is preferable to simply taking the resistive midpoint, see [4], section 4. The results obtained by using this method are shown in figure 6.

It was found that whilst B_{c2} varies strongly with θ_{true} it shows little or no ϕ_{true}-dependence. It is possible to fit the data with the functional form of the predictions of the Ginsburg–Landau anisotropic effective mass approximation [16, 17, 19]:

$$B_{c2}(\theta_{\text{true}}) = \frac{B_{c2\perp}}{\sqrt{\cos^2(\theta_{\text{true}}) + \gamma^{-2}\sin^2(\theta_{\text{true}})}}, \tag{5}$$

in which $B_{c2\perp}$ is the upper critical field when B is directed along the interplane direction and γ is the square root of the ratio of the effective masses for interplane and in-plane motion respectively.

Although it is seen from figure 6 that the data fit reasonably well to the formula, it would not be correct to infer an anisotropy of the effective masses from the values obtained from the fit. This is because the Ginsburg–Landau theory is based on the superconducting state

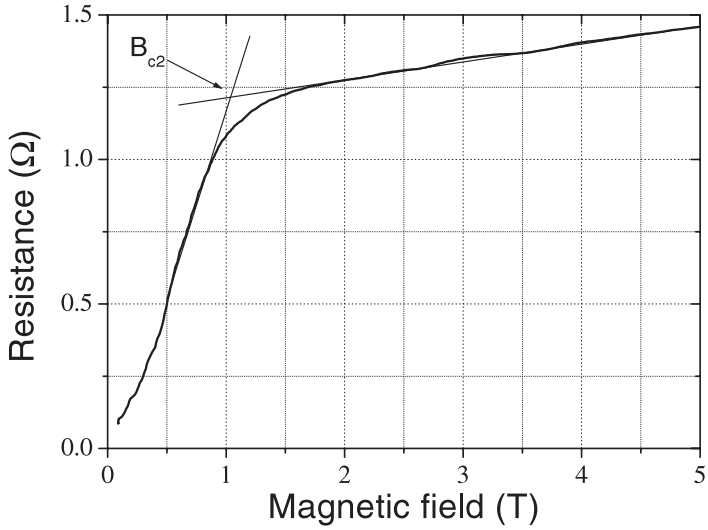

Figure 5. Resistance of a single crystal of $(BEDT\text{-}TTF)_3Cl_2{\cdot}2H_2O$ as function of magnetic field at 14.0 kbar, $T = 0.5$ K and $\theta_{true} = 171°$. The intersection of the straight lines defines B_{c2}.

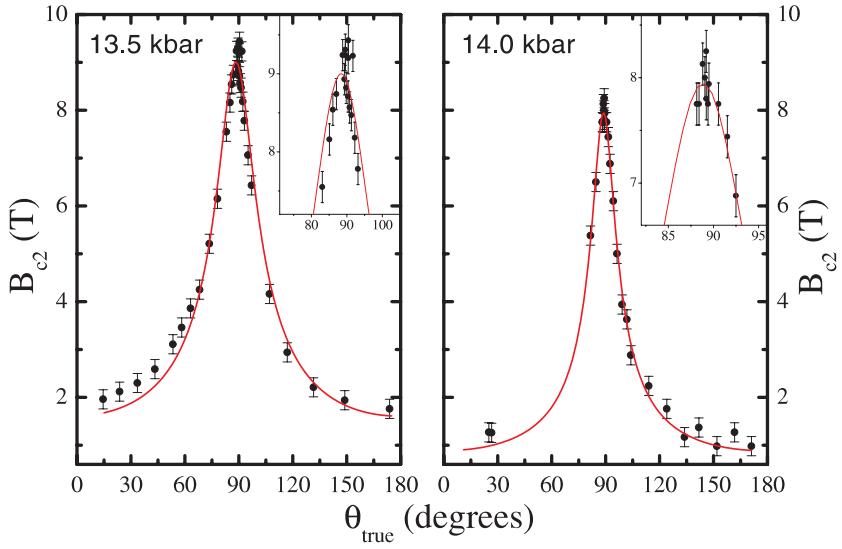

Figure 6. The angular dependence of the upper critical field of $(BEDT\text{-}TTF)_3Cl_2{\cdot}2H_2O$ at 13.5 and 14.0 kbar. The data were taken at several different values of ϕ_{true}. The solid curve is a fit to equation (5) (see text). θ_{true} is the angle between the magnetic field and the normal to the conducting planes.

being destroyed by orbital effects [4]. In the case of highly anisotropic layered materials such as $(BEDT\text{-}TTF)_3Cl_2{\cdot}2H_2O$, the flux lines can become trapped inside the layers when a sufficiently high in-plane magnetic field is applied, and in this situation the upper critical field in the in-plane direction ($B_{c2\|}$) will become very high (for a more complete discussion see [4]). As $B_{c2\|}$ is not particularly large in $(BEDT\text{-}TTF)_3Cl_2{\cdot}2H_2O$ it is assumed that another effect is limiting the superconductivity in the presence of low in-plane fields.

Table 1. Results from the data in figure 6. $B_{c2\perp}$ and $\xi_{\parallel}$ are found by fitting to equation (5) and B_{PPL} is the Pauli paramagnetic limit.

	13.5 kbar	14.0 kbar
T_c (K)	3.5 ± 0.5	2.6 ± 0.5
B_{c2max} (T)	9.2 ± 0.2	8.3 ± 0.2
$B_{c2\perp}$ (T)	1.61 ± 0.2	0.88 ± 0.2
$\xi_{\parallel}$ (Å)	143 ± 18	193 ± 44
$B_{PPL} = 1.84T_c$ (T)	6.0 ± 0.5	4.8 ± 0.5

Despite this failure of Ginsburg–Landau theory to describe the anisotropy of B_{c2}, the functional form of equation (5) is still valid as it is just derived from a vector sum of two competing critical fields and is independent of the mechanism responsible for these critical fields [20]. Thus the γ factor that is found from the fit is in fact just a measure of the critical field anisotropy and is found to be 5.6 ± 0.2 and 9.0 ± 0.3 for 13.5 and 14.0 kbar respectively. In addition, when the field is perpendicular to the conducting planes the critical field is certainly limited by orbital effects and so we can use the fits in figure 6 to obtain valid values for $B_{c2\perp}$ and hence the in-plane coherence length, $\xi_{\parallel}$, using the relation

$$B_{c2\perp} = \frac{\Phi_0}{2\pi\xi_{\parallel}^2}, \tag{6}$$

where Φ_0 is the flux quantum [19]. The values obtained, together with the other results mentioned in this section, are shown in table 1.

One mechanism that might explain the origin of $B_{c2\parallel}$ in (BEDT-TTF)$_3$Cl$_2$·2H$_2$O is the Pauli paramagnetic limit, also known as the Clogston–Chandrasekhar limit [21, 22]. In this case the superconductivity is destroyed by Zeeman splitting of the Cooper pairs at fields above B_{PPL}. For an isotropic, BCS-like superconductor $B_{PPL} = 1.84T_c$ [21]. Applying this to (BEDT-TTF)$_3$Cl$_2$·2H$_2$O we find that $B_{PPL} = 6.0 \pm 0.5$ and 4.8 ± 0.5 T for 13.5 and 14.0 kbar respectively. It is seen from figure 6 and table 1 that the maximum B_{c2}-values are significantly larger than these values for both pressures. It is apparent that this simple isotropic, BCS-like analysis is not able to describe the in-plane upper critical field in (BEDT-TTF)$_3$Cl$_2$·2H$_2$O at these pressures and another mechanism needs to be invoked in order to explain the data.

Similar results were found for the organic superconductors (TMTSF)$_2$PF$_6$ [23] and κ-(BEDT-TTF)$_2$Cu(NCS)$_2$ [18, 19]. In their study Lee *et al* [23] show that the superconducting state in (TMTSF)$_2$PF$_6$ at a certain pressure persists in applied in-plane fields of up to 9 T, far exceeding the expected Pauli paramagnetic limit, although in (TMTSF)$_2$PF$_6$ the effect is more pronounced than for (BEDT-TTF)$_3$Cl$_2$·2H$_2$O due to the lower critical temperature ($T_c = 1.2$ K). Lee *et al* also observe a marked ϕ-dependence of the in-plane upper critical field, which is not observed in the material studied here. The conclusion of [23] is that (TMTSF)$_2$PF$_6$ is a strong contender for triplet Cooper pairing. In the case of κ-(BEDT-TTF)$_2$Cu(NCS)$_2$, Zuo *et al* claim that the B_{PPL} derived from thermodynamic arguments is much bigger than the value suggested by BCS theory [19], whereas Singleton *et al* [18] suggest that the high in-plane critical field is caused by a field-induced transition into a Fulde–Ferrell–Larkin–Ovchinnikov (FFLO) superconducting state. The FFLO state occurs when quasiparticles with opposite spin, whose Fermi surfaces are split by the magnetic field, form Cooper pairs with non-zero momentum [24]. These examples highlight some of the possible mechanisms that enhance the in-plane critical field with respect to B_{PPL} in organic superconductors; however, none of these mechanisms can be definitively attributed to (BEDT-TTF)$_3$Cl$_2$·2H$_2$O without further extensive measurements.

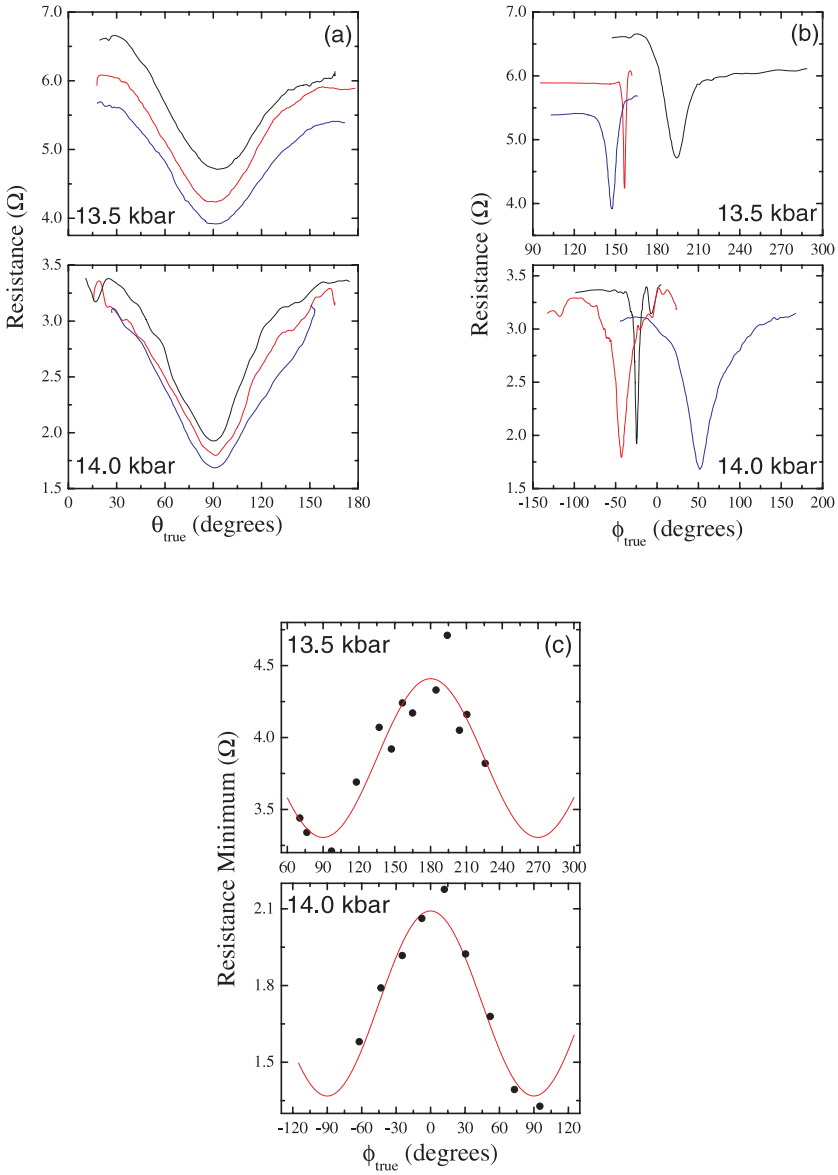

Figure 7. (a) Interlayer magnetoresistance of (BEDT-TTF)$_3$Cl$_2$·2H$_2$O as a function of $\theta_{\rm true}$ with $B = 30$ T and $T = 0.5$ K at 13.5 and 14.0 kbar. The three different curves are from three different values of the measured ϕ-angle. (b) The same curves as in (a) shown as a function of $\phi_{\rm true}$. (c) The points represent the resistance minima at $\theta_{\rm true} = 90°$ as a function of $\phi_{\rm true}$. The solid curves are fits to a single cosine function with twofold symmetry.

3.2. Angle dependence of the magnetoresistance

Figure 7(a) shows the interlayer magnetoresistance of (BEDT-TTF)$_3$Cl$_2$·2H$_2$O as a function of $\theta_{\rm true}$ in a steady magnetic field of 30 T. Three different values of the measured ϕ-angle are shown.

As already mentioned in section 2.3, it is difficult in such a measurement to separate the effects due to the azimuthal and out-of-plane angles, because as the sample is rotated in the

$\theta_{\rm true}$-direction, $\phi_{\rm true}$ also changes to an extent determined by the magnitude of the offset angle ϵ. In light of this, figure 7(b) shows the same curves as in figure 7(a) but as function of $\phi_{\rm true}$. Owing to the mixing of angles it is not easy to obtain a functional form for the magnetoresistance, but what is clear from the figure is that there is a minimum in resistance at $\theta_{\rm true} = 90^\circ$ and a maximum when the field component in the interlayer direction takes its maximum value. This behaviour is contrary to the expectation that the magnetoresistance should be a minimum when the magnetic field is parallel to the applied current and a maximum when the field and current are perpendicular, as expected from semiclassical transport theory [25]. However the situation is not without precedent in organic molecular crystals. $(TMTSF)_2PF_6$ at 9.8 kbar [26, 27], $(TMTSF)_2ClO_4$ [28] and τ-[P-(S, S)-DMEDT-TTF]$_2$(AuBr)(AuBr)$_y$ [29] all show this type of angle dependence in the interlayer resistance, and in all three cases it is attributed to the interlayer transport being incoherent in nature, i.e. the Fermi surface is a two-dimensional object that exists only in the conducting layers and the charge-carriers must undergo some kind of hopping mechanism to move from layer to layer.

This situation can arise when an in-plane magnetic field is applied to a sample even if the interlayer transport is coherent to begin with. Increasing the in-plane component of the field reduces the semiclassical width of the interplane component of the quasiparticle orbits. At a certain field this width will become less than the interlayer spacing, at which point the quasiparticles are essentially confined to a single conducting layer. This is the single-body confinement argument of Osada *et al* [28] and their in-plane confinement field is given by $B_{\rm conf} = 4t_\perp/ev_{\rm F}l_c$, where $t_\perp$ is the interlayer transfer integral, $v_{\rm F}$ is the Fermi velocity and l_c is the interlayer spacing. Typical values of $t_\perp$ and $v_{\rm F}$ for BEDT-TTF salts are 0.1 meV and 50 km s^{-1} respectively [4, 5] and, for (BEDT-TTF)$_3$Cl$_2$·2H$_2$O, $l_c = 15.03$ Å. Hence $B_{\rm conf} \approx 5$ T. For inclined fields it is $B \sin\theta_{\rm true}$ that determines the in-plane component, thus in fields of 30 T (as in figure 7) the interlayer transport should be incoherent for $\theta_{\rm true} \gtrsim 10^\circ$.

Strong and Clarke [30, 31] argue that the crossover from three- to two-dimensional transport can occur at much lower values of the in-plane field. Their reasoning is that the strong-correlation effects in highly anisotropic materials can be enhanced by a small in-plane field that introduces inelasticity into the interlayer transport and effectively reduces the coherent interlayer transfer integral to zero.

Whatever the cause of the incoherent interlayer transport, the result is the same: the semiclassical transport theory breaks down and the magnetoresistance depends only on the interlayer component of the magnetic field, $B\cos\theta_{\rm true}$. This would account for the data of figure 7(a).

Figure 7(c) shows the $\phi_{\rm true}$-dependence of the minimum in resistance that occurs at $\theta_{\rm true} = 90^\circ$. The solid curve is a fit of the data to a cosine function with twofold symmetry. By considering the Fermi surface shown in figure 2 it is seen that applying the magnetic field along the Γ–Y (or b^*) direction maximizes the Lorentz force acting on both the Q1D and Q2D carriers for in this direction the field is perpendicular to the Q1D carrier velocity and also to the *maximum* of the Q2D electron velocity. This is essentially the same as the argument employed by Hussey *et al* [32] to describe the behaviour of the 'high-T_c' compound $YBa_2Cu_4O_8$. Here they conclude that the Q1D carriers dominate the interlayer resistance. This may also be true in the case of (BEDT-TTF)$_3$Cl$_2$·2H$_2$O, but the possible presence of the elongated Fermi surface pocket means that the contribution from the Q2D carriers cannot be neglected. We can, however, conclude that the b^*-direction corresponds to $\phi_{\rm true} = 0^\circ$.

3.3. Magnetoresistance at 13.5 kbar

The magnetoresistance of (BEDT-TTF)$_3$Cl$_2$·2H$_2$O at 13.5 kbar is shown in figure 8. The curves are data taken at different angles, the $\theta_{\rm true}$ angle varying from 23.7° to 83.1° and the $\phi_{\rm true}$ angle

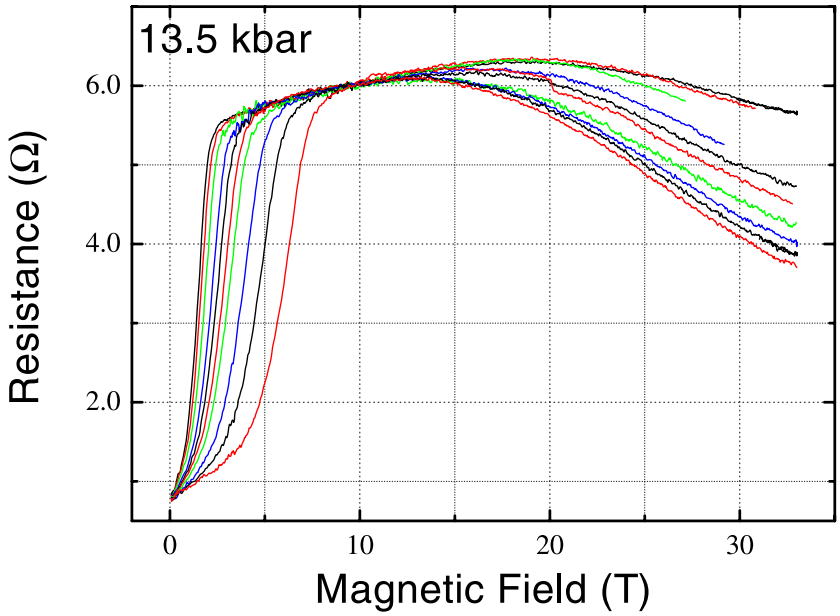

Figure 8. Interlayer magnetoresistance of $(BEDT\text{-}TTF)_3Cl_2{\cdot}2H_2O$ at 13.5 kbar and 0.5 K. The different lines correspond to different values of θ_{true} and ϕ_{true}. The (θ_{true}, ϕ_{true}) values are, starting with the curve having the highest resistance at 33 T: (23.7°, 160.9°); (33.6°, 156.3°); (43.4°, 153.6°); (53.4°, 151.7°); (58.2°, 151.0°); (63.2°, 150.3°); (68.2°, 149.7°); (73.6°, 149.08°); (78.1°, 148.6°) and (83.1°, 148.1°). Note that although the θ_{true} values range widely, the ϕ_{true} values vary only by about 12°.

varying very little. It is seen that for θ_{true} angles away from 90° the data in fields up to 15 T resemble the saturating magnetoresistance observed by Lubczynski *et al* [10]. This suggests that we are in the region of the phase diagram proposed in that paper where the CDW is not yet fully suppressed and the transport is dominated by the Q2D carriers (i.e. in the superconducting state, just below P_c, see figure 1). At fields greater than 15 T the magnetoresistance becomes negative. For each of the curves θ_{true} is a constant and so the data in figure 8 cannot be explained by the $B\cos\theta_{true}$ dependence derived from the incoherent interlayer transport models of Osada or Strong and Clarke [28, 30, 31].

3.3.1. Comparison with other materials. It is worthwhile making a diversion at this point to discuss the results found in a few other organic conductors, as it may help to shed some light on the situation in hand. It has already been mentioned that at 9.8 kbar the behaviour of $(TMTSF)_2PF_6$ can be explained in terms of the Strong and Clarke many-body confinement picture [30, 31]. This leads to a decoupling of the conducting layers and a $B\cos\theta$ dependence of the interlayer magnetoresistance [26]. However, at lower pressures (6–8.3 kbar) all evidence for this decoupling is lost and the angle-dependence of the interlayer magnetoresistance follows the semi-classical $B\sin\theta$ result [33]. This implies that the layers are coupled better at lower pressures, which is contrary to the expectation that a higher pressure will cause the electron orbitals to overlap to a greater degree and thus *increase* the coherence in the interlayer direction. Another curious matter concerns the magnetoresistance of $(TMTSF)_2PF_6$ at these low pressures when an in-plane field is applied parallel to the Q1D Fermi surface sheets. In this case the

resistance saturates in field of up to 7 T [33]. This contradicts the predictions of *both* the semi-classical and the Strong and Clarke theories, in which a non-saturating and diverging magnetoresistance are expected respectively. This is itself similar to the results found for $(TMTSF)_2ClO_4$, which is the material used to illustrate Osada's single-body confinement effect [28]. In the latter material Naughton *et al* [34] again noted a saturating magnetoresistance and in fact used high fields to show that there is an onset of negative magnetoresistance at around 28 T. Another negative magnetoresistance is recorded in the material τ-[P-(S, S)-DMEDT-TTF]$_2$(AuBr)$(AuBr)_y$ of [29].

Thus it is seen that the effects observed in $(BEDT\text{-}TTF)_3Cl_2{\cdot}2H_2O$ are not unique. However this brings us no closer to an explanation. In the much measured $(TMTSF)_2PF_6$ theoretical considerations predict a field induced re-entrance of the superconductivity [35]. However in $(BEDT\text{-}TTF)_3Cl_2{\cdot}2H_2O$ there is no evidence to suggest that the observed down-turn of the magnetoresistance can be attibuted to a re-entrance. Moreover, the predicted restoration of the superconductivity in anisotropic systems occurs only in those that exhibit spin-triplet superconductivity and seems to require a purely Q1D system or a careful alignment of the applied magnetic field parallel to the Q1D Fermi surface sheets [23, 35, 36], whereas Q2D carriers have been observed in $(BEDT\text{-}TTF)_3Cl_2{\cdot}2H_2O$ [10], and it is seen from figure 8 that the negative magnetoresistance occurs for many different field directions.

3.3.2. The effects of Anderson localization. The most likely mechanism responsible for the negative magnetoresistance at high magnetic fields, at least in $(BEDT\text{-}TTF)_3Cl_2{\cdot}2H_2O$, is the presence of Anderson localization within the conducting planes [37, 38]. According to Fukuyama and Yosida the variable-range hopping mechanism responsible for conduction in the localized regime would give rise to a large negative magnetoresistance [37]. The explanation is that a random potential produces the Anderson localized states, i.e. states below the mobility edge, E_c. If the Fermi energy, E_F, lies below E_c then at low temperatures conduction is only possible by means of variable-range hopping. Application of a magnetic field leads to a Zeeman splitting of the electronic energy levels, and with further increases in field the difference between E_c and energy of an electron with spin parallel to the magnetic field decreases, leading to an increase in the conductivity. This effect will be enhanced when $E_c - E_F$ is small, such as in the vicinity of a metal–nonmetal transition [38] (like that due to the destruction of the CDW in $(BEDT\text{-}TTF)_3Cl_2{\cdot}2H_2O$). The conductivity resulting from these considerations would have the form [37]

$$\sigma \propto \exp\left[\left(\frac{T_0}{T}\right)^{1/2}\left\{1-\left(1-\frac{1}{2}g\mu_B B/(E_c-E_F)\right)^{\beta d/n}\right\}\right] + \exp\left[\left(\frac{T_0}{T}\right)^{1/2}\left\{1-\left(1+\frac{1}{2}g\mu_B B/(E_c-E_F)\right)^{\beta d/n}\right\}\right]. \tag{7}$$

Here T_0 is a characteristic temperature obtained from the temperature dependence of the conductivity, d is the dimensionality of the system, n is an integer (which for the simplest model is equal to $d+1$ [38]), g is the effective g-factor (which is assumed to be $\simeq 2$), μ_B is the Bohr magneton and $\beta \simeq 1$. Following the analysis of Fukuyama and Yosida it is noted that because of the relationship between d and n, $\beta d/n$ is always of the order of 1, and equation (7) is not particularly sensitive to its precise value. Thus we choose $\beta d/n = 1$ for a fit to the magnetoresistance data of figure 8. The result of the fitting is shown in figure 9 and it is seen that the fit is good at all angles. A value for T_0 can be obtained from the temperature dependence of the resistance, which follows the form $R \propto \exp[(T_0/T)^{1/n}]$ (although in $(BEDT\text{-}TTF)_3Cl_2{\cdot}2H_2O$ this is complicated by the CDW and superconducting transitions). Using this

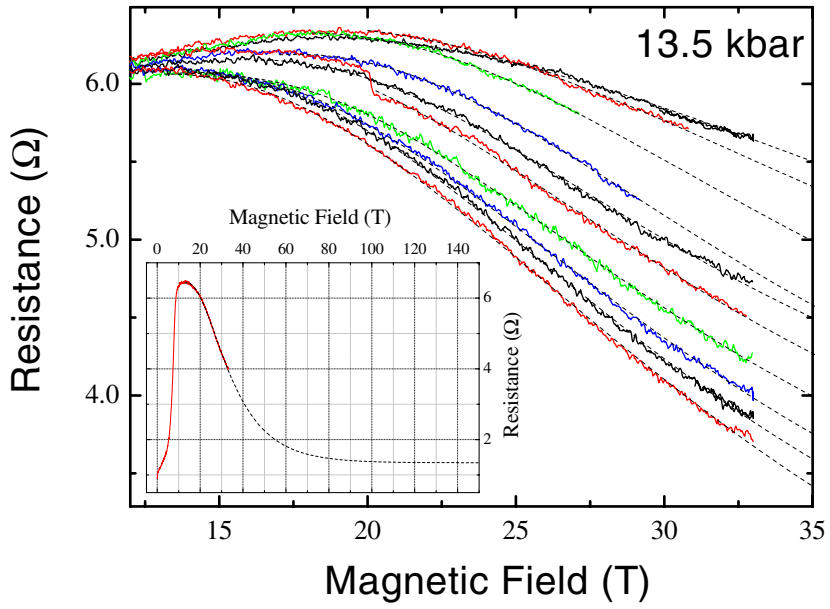

Figure 9. The solid curves are the same data as in figure 8 and the dotted curves are fits using the form of equation (7). The inset shows the data for a field sweep at 0.5 K with $\theta_{\text{true}} = 89.8°$, and the corresponding fitted curve extrapolated to high magnetic fields. The extrapolation of the Anderson localization model to very high fields is shown for illustrative purposes only.

value, together with the results obtained from the fit for data with an almost exactly in-plane field, $E_c - E_F$ is estimated to be about 6 meV. When the Zeeman energy ($\frac{1}{2}g\mu_B B$) of an electron approaches $E_c - E_F$ the electrons will no longer be confined to the localized states and the negative magnetoresistance is expected to saturate. This can be seen in the inset of figure 9 which shows the fitted magnetoresistance saturating in a magnetic field of about 100 T which corresponds to the estimated Zeeman energy of 6 meV.

Another prediction of the Anderson localization model of Fukuyama and Yosida [37] is the existence of a critical applied electric field, proportional to $T^{4/3}$, above which the conduction can no longer be considered as ohmic. At the low temperatures used here the applied current produces an electric field across the sample well below this critical value. However at higher temperatures the resistance of the sample increases by several orders of magnitude and this could lead to the critical electric field being exceeded when even reasonably small currents are applied. This might account for the region of non-ohmic conductivity observed by Lubczynski *et al* between 150 and 30 K at ambient pressure.

If this Anderson localization effect is indeed responsible for the observations in (BEDT-TTF)$_3Cl_2{\cdot}2H_2O$, then the mechanism responsible for introducing disorder and randomizing the potential must be considered. Ulmet *et al* discuss the shape of the anion as a possible source in the family of organic conductors $(DMtTSF)_2X$, as they only observe the effects of localization in crystal with a tetrahedral anion [39]. However a much more likely candidate in the case of (BEDT-TTF)$_3Cl_2{\cdot}2H_2O$ is the CDW itself, which at 13.5 kbar has not yet been fully suppressed. The presence of the density wave could introduce scattering centres in the conducting planes and hence lead to localization. It is also possible that even low levels of intrinsic disorder due to impurities or vacancies could have a considerable effect on the conduction properties of crystalline organic conductors of reduced dimensionality. It has recently been suggested that

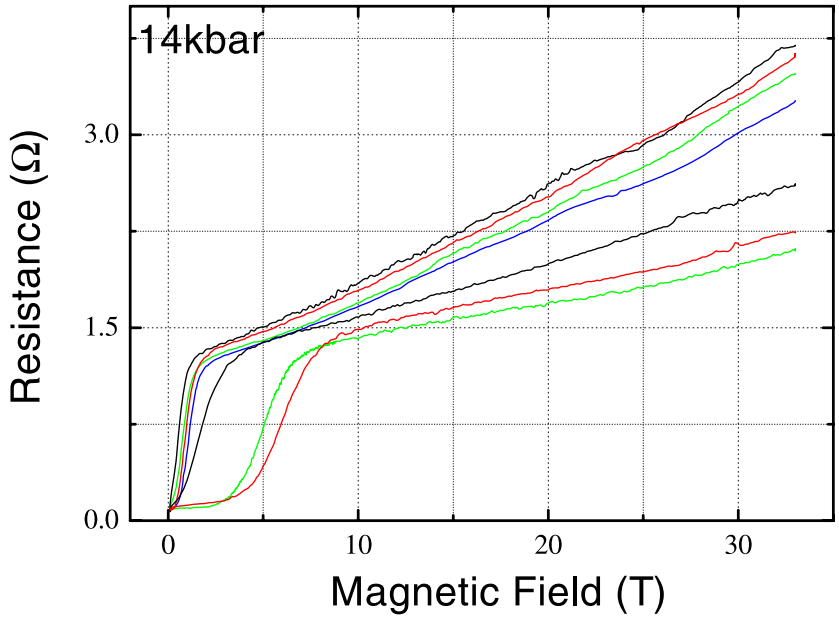

Figure 10. Interlayer magnetoresistance of (BEDT-TTF)$_3$Cl$_2$·2H$_2$O at 14.0 kbar and 0.5 K. The different lines correspond to different values of $\theta_{\rm true}$ and $\phi_{\rm true}$. The ($\theta_{\rm true}$, $\phi_{\rm true}$) values are, starting with the curve having the highest resistance at 33 T: (151.9°, 1.1°); (141.9°, 358.5°); (26.6°, 352.0°); (25.6°, 349.8°); (104.1°, 354.0°); (89.2°, 352.9°); (84.6°, 352.5°).

the anomalously broad superconducting transition in such crystals can be accounted for by very small impurity concentrations ($\lesssim$0.2%) [40].

3.4. Magnetoresistance at 14.0 kbar

Figure 10 shows the magnetoresistance of (BEDT-TTF)$_3$Cl$_2$·2H$_2$O at the slightly higher pressure of 14.0 kbar. It is seen that the magnetoresistance is no longer negative, and is in fact positive and non-saturating at all angles. It is also seen that for field sweeps with $\theta_{\rm true}$ away from 90°, low-amplitude, low-frequency SdH oscillations are superposed over the background magnetoresistance. In the analysis of Lubczynski *et al* [10] this implies that the sample is in the region of the phase diagram where the CDW has been completely suppressed and the transport is dominated by the liberated Q1D carriers (i.e. in the superconducting state, just above $P_{\rm c}$, see figure 1). The background magnetoresistance for all angles can be fitted well with a $B^{3/2}$ dependence, which is the result found by Strong and Clarke [31] in (TMTSF)$_2$PF$_6$ and described using their incoherent transport model [30].

The fact that the negative magnetoresistance due to Anderson localization is not observed at 14.0 kbar is unsurprising if we attribute the random potential that causes the localization to the CDW fluctuation. Here the CDW is fully suppressed and so localization effects are not expected. Even if the Anderson localization is not directly caused by the CDW we might expect the liberation of the Q1D carriers to increase the carrier density to such an extent that any scattering centres present are effectively screened from the charge carriers and the variable-range hopping does not occur. Thus at 14.0 kbar the angle-dependent and field-dependent magnetoresistance imply an interlayer incoherence in which Anderson localization is no longer an important consideration.

3.5. P_c and the superconducting state

If the Anderson localization model suggested here is to be applied to (BEDT-TTF)$_3$Cl$_2$·2H$_2$O it is necessary to reclarify the significance of the critical pressure, P_c. In section 1 P_c was defined as the pressure at which the CDW transition temperature approaches 0 K, and hence at low temperatures it is also the pressure that separates the regions of saturating and non-saturating magnetoresistance in fields of up to 15 T. Lubczynski *et al* [10] attributed these regions to the conduction being dominated by Q2D and Q1D carriers respectively. However in the present analysis the saturating magnetoresistance is merely a precursor to a negative magnetoresistance caused by Anderson localization. Thus it is not possible to deduce the nature of the dominant carriers below P_c, and the dotted line in figure 1, which intercepts the pressure axis at P_c, merely separates the region where the effects of the localization are observed and the region at higher pressure where they are not. In the region above P_c the existence of the Q2D carriers is implied by the SdH oscillations observed at high fields.

It should be noted that P_c for the sample discussed in this paper is approximately 1 kbar higher than the value obtained by Lubczynski *et al* [10]. However if, as suggested, the low temperature electronic properties in the region just below P_c are dominated by random localization effects then a certain degree of sample dependence is to be expected.

Lubczynski *et al* also suggest that the fact that the onset of superconductivity coincides with the appearance of the saturating magnetoresistance implies that it is Q2D carriers that form the superconducting pairs. Extending this idea to the model presented here suggests that there is a connection between the superconducting state and the Anderson localization. This theory is undermined by the fact that the superconductivity exists in the region above P_c where the effects of localization are no longer observed. In fact it seems much more likely that the onset of both the superconductivity and the negative magnetoresistance occurs in the region close to the complete suppression of the CDW where there are only just enough free carriers available to observe any type of electrical conduction effect whatsoever.

4. Conclusions

In summary, we have measured the angle-dependent interlayer magnetoresistance of the pressure-induced organic superconductor (BEDT-TTF)$_3$Cl$_2$·2H$_2$O at two pressures: one at which there is evidence for a CDW state, and one at which this CDW is completely suppressed. At both pressures the in-plane upper critical field exceeds the Pauli paramagnetic limit and an incoherent interlayer transport mechanism is observed in the presence of an in-plane magnetic field component. At the lower pressure a negative magnetoresistance is seen, indicating that the transport is dominated by variable-range hopping caused by a degree of Anderson localization in the highly conducting organic layers. At the higher pressure the magnetoresistance becomes positive and the effects of Anderson localization are no longer observed following the complete suppression of the CDW state. This implies a strong connection between the CDW and the Anderson localization.

The Anderson localization model of Fukuyama and Yosida [37] is the currently the only mechanism that can explain all the effects observed in (BEDT-TTF)$_3$Cl$_2$·2H$_2$O.

We also note the similarities in physical properties of this material and several other organic molecular crystals, in particular τ-[P-(S, S)-DMEDT-TTF]$_2$(AuBr) (AuBr)$_y$ [29], (TMTSF)$_2$ClO$_4$ [34] and (TMTSF)$_2$PF$_6$ [33], and suggest that it is possible that the Anderson localization model described here could be used to explain the negative and saturating magnetoresistances observed in these materials.

Acknowledgments

This work is supported by the EPSRC (UK) and the CNRS (France). NHMFL is supported by the US Department of Energy (DoE), the National Science Foundation and the State of Florida. We thank Steve Blundell for stimulating discussions.

Note added in proof. We note that the phase diagram of the material discussed here agrees with the theoretical phase diagram shown in figure 1 of [41]. In this article the authors apply slave-boson theory to a layered molecular crystal with charge ordering and superconducting interactions. Applying pressure to the material considered in the present paper will reduce the ratio V/t, which is on the x-axis of the figure in [41], thus the state of the system will move to the left of the phase diagram.

References

[1] Mori T 1998 *Bull. Chem. Soc. Japan* **71** 2509
Mori T, Mori H and Tanaka S 1999 *Bull. Chem. Soc. Japan* **72** 179
Mori T 1999 *Bull. Chem. Soc. Japan* **72** 2011
[2] Mckenzie R H 1997 *Science* **278** 820
[3] Singleton J 2000 *Rep. Prog. Phys.* **63** 1111
[4] Singleton J and Mielke C 2002 *Contemp. Phys.* **43** 150
[5] Singleton J, Goddard P A, Ardavan A, Harrison N, Blundell S J, Schlueter J A and Kini A M 2002 *Phys. Rev. Lett.* **88** 7001 and references therein
[6] Whangbo M H, Ren J, Kang D B and Williams J M 1990 *Mol. Cryst. Liq. Cryst.* **181** 17
[7] Mori T and Inokuchi H 1987 *Chem. Lett.* **1987** 1657
[8] Obertelli S D, Marsden I R, Friend R H, Kurmoo M, Rosseinsky M J, Day P, Pratt F and Hayes W 1990 *Proc. ISSP Int. Symp. on the Physics and Chemistry of Organic Superconductors (Springer Proceedings in Physics vol 51)* ed G Saito and S Kagoshima (Berlin: Springer) p 181
[9] Gaultier J, Hébrard-Bracchetti S, Guionneau P, Kepert C J, Chasseau D, Ducasse L, Barrans Y, Kurmoo M and Day P 1999 *J. Solid State Chem.* **145** 496
[10] Lubczynski W, Demishev S V, Singleton J, Caulfield J M, du Croo de Jongh L, Kepert C J, Blundell S J, Hayes W, Kurmoo M and Day P 1996 *J. Phys.: Condens. Matter* **8** 6005
[11] Kurmoo M, Rosseinsky M J and Day P 1988 *Synth. Met.* **27** A425
[12] Rosseinsky M J, Kurmoo M, Talham D R, Day P, Chasseau D and Watkin D 1988 *J. Chem. Soc. Chem. Commun.* **1988** 88
[13] Tozer S W 2002 at press
[14] Eremets M 1996 *High Pressure Experimental Methods* (Oxford: Oxford University Press) p 172
[15] Yen J and Nichol M 1992 *J. Appl. Phys.* **72** 5535
[16] Tinkham M 1996 *Introduction to Superconductivity* 2nd edn (New York: McGraw-Hill)
[17] Nakamura T, Komatsu T, Saito G, Osada T, Kagoshima S, Noboru M, Kato K, Maruyama Y and Oshima K 1993 *J. Phys. Soc. Japan* **62** 4373
[18] Singleton J, Symington J A, Nam M-S, Ardavan A, Kurmoo M and Day P 2000 *J. Phys.: Condens. Matter* **12** L641
[19] Zuo F, Brooks J S, McKenzie R H, Schlueter J A and Williams J M 2000 *Phys. Rev.* B **61** 750
[20] Nam M-S, Symington J A, Singleton J, Blundell S J, Ardavan A, Perenboom J A A J, Kurmoo M and Day P 1999 *J. Phys.: Condens. Matter* **11** L477
[21] Clogston A M 1962 *Phys. Rev. Lett.* **9** 266
[22] Chandrasekhar B S 1962 *Appl. Phys. Lett.* **1** 7
[23] Lee I J, Chaikin P M and Naughton M J 2000 *Phys. Rev.* B **62** R14 669
[24] Fulde P and Ferrell R A 1964 *Phys. Rev.* A **135** 550
Larkin A I and Ovchinnikov Yu N 1964 *Zh. Eksp. Teor. Fiz.* **47** 1136 (Engl. transl. 1965 *Sov. Phys.–JETP* **20** 762)
[25] See for example
Ashcroft N W and Mermin A D 1976 *Solid State Physics* (Philadelphia, PA: Saunders) p 233
or
Singleton J 2001 *Band Structure and Electronic Properties of Solids* (Oxford: Oxford University Press) p 136
[26] Danner G M and Chaikin P M 1995 *Phys. Rev. Lett.* **75** 4690
[27] Chashechkina E I and Chaikin P M 1998 *Phys. Rev. Lett.* **80** 2181

[28] Osada T, Kami N, Kondo R and Kagoshima S 1999 *Synth. Met.* **103** 2024
[29] Storr K, Balicas L, Brooks J S and Graf D 2001 *Phys. Rev.* B **64** 045107
[30] Clarke D G and Strong S P 1997 *Adv. Phys.* **46** 545
[31] Strong S P, Clarke D G and Anderson P W 1994 *Phys. Rev. Lett.* **73** 1007
[32] Hussey N, Kibune M, Nakagawa H, Miura N, Iye Y, Takagi H, Adachi S and Tanabe K 1998 *Phys. Rev. Lett.* **80** 290
[33] Lee I J and Naughton M J 1998 *Phys. Rev.* B **58** R13 343
[34] Naughton M J, Lee I J, Chaikin P M and Danner G M 1997 *Synth. Met.* **85** 1481
[35] Lebed A G 1986 *Sov. Phys.–JETP* **44** 114
Dupuis N, Montambaux G and Sá de Melo C A R 1993 *Phys. Rev. Lett.* **70** 2613
Dupuis N 1995 *Phys. Rev.* B **51** 9074
[36] Chashechkina E I, Lee I J, Brown S E, Chow D S, Clark W G, Naughton M J and Chaikin P M 2001 *Synth. Met.* **119** 13
[37] Fukuyama H and Yosida K 1979 *J. Phys. Soc. Japan* **46** 102
[38] Kobayashi N and Muto Y 1979 *Solid State Commun.* **30** 337 and references therein
[39] Ulmet J P, Bachère L, Askenazy S and Ousset J C 1988 *Phys. Rev.* B **38** 7782
[40] Singleton J, Harrison N, Mielke C H, Schlueter J A and Kini A M 2001 *J. Phys.: Condens. Matter* **13** L899
[41] Mexino J and McKenzie R H 2001 *Phys. Rev. Lett.* **87** 237002